



A Review of the Influence of Microscopic Characteristics on the Progressively Brittle Failure of Foliated Rocks Subjected to Compression Loading

Xiaomeng Yin · Aiming Zhang · Xia Zhang

Received: 24 July 2021 / Accepted: 21 November 2021 / Published online: 30 November 2021
© The Author(s), under exclusive licence to Springer Nature Switzerland AG 2021

Abstract The progressively brittle failure of foliated rocks involving the initiation, propagation, and aggregation modes is closely related to the microscopic characteristics of these rocks. For this particular type of rock, the phyllosilicate minerals and microcracks in the microstructure have a certain preferred orientation, and the minerals display typical spatial arrangement features. Moreover, phyllosilicate minerals exhibit deformation behaviors such as dislocation slip, plastic kinking, and fracture failure during the compression process, which play an important role in the evolution of rock cracks. In addition, directional microcracks are primarily distributed at the edge of phyllosilicate minerals, and these significantly impact the accumulation of rock damage. The oriented phyllosilicate minerals and the microcracks jointly constitute the weak layer of the foliated rock. When loaded with the weak layer in different directions, the rock will show anisotropy at the micro and macro levels. Based on previous studies, this paper summarizes and analyzes

the microscopic mechanism and crack evolution law of foliated rock, aiming to expand the understanding of the correlation of the microscopic characteristics with the macro- and mesomechanical behavior of this kind of anisotropic rock, which may significantly lead to further studies on rock anisotropy.

Keywords Foliated rock · Anisotropy · Phyllosilicate mineral · Directional microcrack

List of Symbols

σ_{cc}	Crack closure stress
σ_{ci}	Crack initiation stress
σ_{cd}	Crack damage stress
σ_f	Peak stress
α	The weak surface angle
σ_3	Minimum principal stress
β	The angle between the kink zone boundary and the cleavage plane of the phyllosilicate mineral
w	The width of the kink belt
LMC	Linear mica continuity
LMC_{max}	The maximum linear mica continuity

X. Yin (✉)
College of Intelligent Construction, Wuchang University of Technology, Wuhan 430223, China
e-mail: xiaomenghehe@163.com

X. Yin · A. Zhang · X. Zhang
College of Architecture and Civil Engineering, Xinyang Normal University, Xinyang 464000, China
e-mail: aimingzhang21@163.com

X. Zhang
e-mail: zxxynu@163.com

1 Introduction

The macroscopic failure of rock involves the process of crack initiation, propagation, and aggregation

(Olsson et al. 1976), which is consistently accompanied by the plastic deformation and fracture failure of mineral particles (Powell 1977; Passchier et al. 2005). In foliated rocks, the deformation and failure of such minerals and the development of cracks exhibit the loading orientation effect, essentially leading to the anisotropic behaviors of rocks at the micro and macro levels. As typical representatives of foliated rocks, phyllite, schist, and gneiss are widely distributed in nature. Additionally, these rocks have inherently weak planes such as schistosity and gneissosity, microscopically caused by the arrangement of specific minerals and microcracks. These micro-weaknesses have a significant “guide effect” on the initiation, propagation, and aggregation of cracks, controlling the foliated rock specimens in the accumulation of microscopic damage along the weak surface throughout the loading process (Rawling et al. 2002).

Figure 1 illustrates the typical stress–strain curve of the pre-peak section of the compressed brittle rocks. According to the development and evolution of original defects and new cracks, the deformation and failure of the compressed rock can be divided into four stages: crack closure, linear elastic deformation, crack propagation, and crack aggregation. When the brittle rock specimen is subjected to uniaxial compression, it first undergoes the crack closure stage, in which the original microcracks in the opening state are compressed and closed, resulting in the appearance of an upward bending curve section in the stress–strain curve (Yu 2016). In addition, the transverse strain curve and the volumetric strain curve begin to increase slowly. When the axial stress reaches σ_{cc} (crack closure stress), the specimen enters the linear elastic deformation stage, in which the axial stress–strain

curve appears as an approximately straight line. When the axial stress reaches σ_{ci} (crack initiation stress), new cracks are initiated, and the specimen enters the crack propagation stage, which is characterized by the stable growth of independent cracks. When the axial stress reaches σ_{cd} (crack damage stress), cracks tend to aggregate and connect, leading to unstable growth (Diederichs et al. 2004). In this stage, the volumetric strain curve begins to reverse, and the rate of lateral strain increase begins to increase significantly. Finally, the axial stress reaches σ_f (peak stress), and the specimen forms a continuous through surface.

During uniaxial compression of brittle rock, the initiation and propagation of new cracks are closely related to the stress level of the rock. At the initiation of new cracks, the critical stress σ_{ci} often reaches $0.2\sigma_f$ – $0.4\sigma_f$, and the stress threshold at which unstable cracks begin to develop is σ_{cd} , which frequently reaches $0.5\sigma_f$ – $0.8\sigma_f$ (Zhang et al. 2011). Among them, σ_{ci} corresponds to the stress point when the axial stress–strain curve starts to show a nonlinear change, which represents the true lower bound of the in situ strength of the material. Then, σ_{cd} is the yield or expansion point of the rock, indicating the long-term strength of the material and representing the true upper bound of its in situ strength (Diederichs et al. 2004). These two stress thresholds divide the crack development status into two stages: propagation and aggregation. For foliated rocks, the crack evolution characteristics and stress thresholds are closely related to the loading orientation, which is controlled by the inherent microstructure.

The microscopic characteristics of foliated rocks are mainly reflected in the distribution and arrangement of phyllosilicate minerals and microcracks. Under metamorphism, the phyllosilicate minerals will appear elongated and have a preferred orientation. In addition, phyllosilicate minerals are often accompanied by several large microcracks. Given their spatial dependence on such minerals, microcracks also have a certain degree of dominant distribution direction (Wang 2014; Yu 2016). The phyllosilicate minerals in foliated rocks include mica, chlorite, talc, kaolinite, montmorillonite, and serpentine, which are weak in nature, strong in toughness, and regularly flaky in morphology, hereinafter referred to as flaky minerals. Other minerals, including quartz, feldspar, calcite, etc., are characterized by greater hardness, poor toughness, and typical plate or granular morphology.

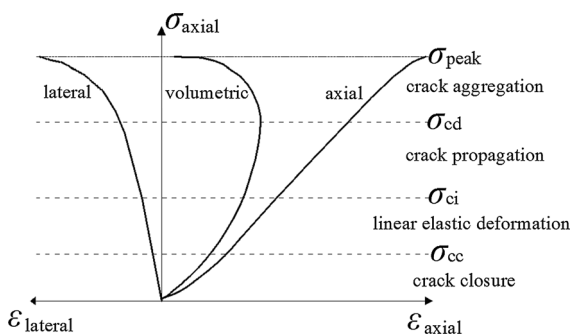


Fig. 1 Pre-peak stress–strain curves of brittle rocks (Diederichs et al. 2004; Zhang et al. 2011)

Therefore, these will be referred to as plate-granular minerals in the following text.

In foliated rocks, the spatial distribution of flaky minerals and plate-granular minerals can be summarized into two types: similarly uniform and interlayer distributions (Fig. 2). The interlayer distribution structure is the product of metamorphic differentiation (Fisher 1970), indicating that the rock underwent significant metamorphism during its formation. Generally, with a low content of flaky minerals, the similarly uniform distribution structure contributes less to the anisotropy (Shea et al. 1993), and the interlayer distribution tends to cause remarkable anisotropy. Cracks in those rocks with structures of similar interlayers more easily expand and aggregate (Wang et al. 2015).

Figure 3 shows the microscopic components of the foliated rock. According to the distribution location, the original cracks in foliated rocks can be divided into flaky mineral edge-oriented directional microcracks, flaky mineral intergranular cracks, boundary cracks of plate-granular minerals, and intragranular cracks of plate-granular minerals. Moreover, the ability of flaky minerals to resist deformation and failure essentially depends on the angle between the maximum principal stress and the weak surface (Shea et al. 1993). To compare the findings of previous studies, the angle of the weak plane is defined as the angle between the maximum principal stress and the dominant direction of flaky minerals and microcracks (Fig. 4).

Since the development of cleavage in different flaky minerals is not the same, to better explain the influence of the weak surface, this paper selects the more common mica with extremely complete

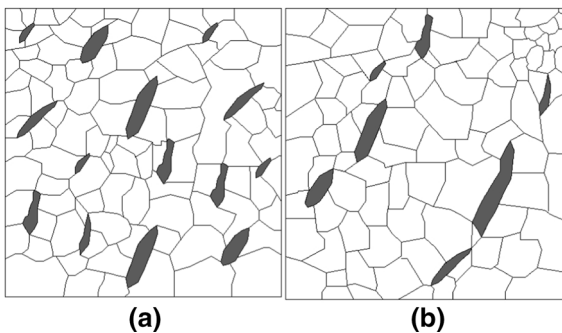


Fig. 2 Microscopic spatial distribution state. **a** The similarly uniform distribution; **b** The similar interlayer distribution (black represents flaky minerals, white represents plate-granular minerals)

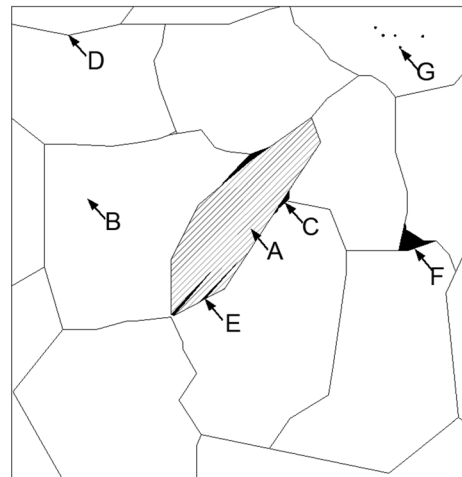


Fig. 3 Microscopic components (A represents flaky mineral, B represents plate-granular mineral, C represents directional microcrack, D represents plate-granular mineral boundary, E represents flaky mineral intergranular crack, F represents boundary crack of plate-granular mineral, G represents intragranular original defect of plate-granular mineral)

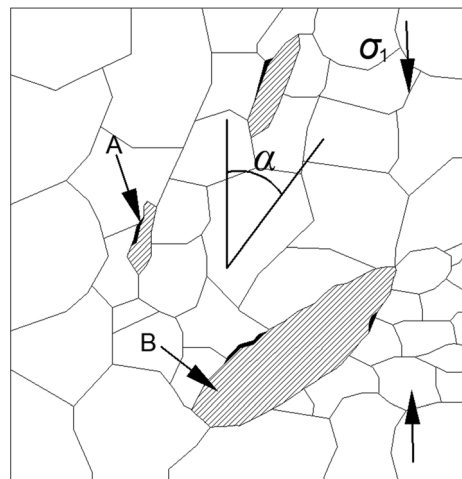


Fig. 4 Definition of the weak side angle (A represents directional microcrack, B represents flaky cleavage surface)

cleavage characteristics as the representative of flaky minerals. This paper summarizes domestic and foreign research on the correlation between microscopic characteristics and the mode of initiation, propagation, and aggregation of cracks in compressed foliated rocks. This greatly promotes the study of the anisotropy of foliated rocks.

2 Crack Initiation Mode

2.1 Control of Flaky Minerals

During the compression of foliated rock specimens, three microscopic deformation behaviors of a single mica can be observed, specifically dislocation slip, plastic kink, and fracture failure (Kronenberg et al. 1990; Kanaori et al. 1991; Mares et al. 1993; Rawling et al. 2002), corresponding to the three types of cracks under the control of flaky minerals.

2.1.1 Dislocation Slip

The mechanism of dislocation slip deformation is that the shear force in the mica crystal exceeds the maximum friction force provided by the decoupling surface, causing relative sliding. Consequently, it leads to a high concentration of local stress at the mica tip. Figure 5 emphasizes that when the stress exceeds the tensile strength of plate-granular minerals, tensile cracks will germinate. Additionally, the sliding initiation mechanism is similar to that of wing cracks (Gottschalk et al. 1990).

Scholars measured the friction coefficient of this type of cleavage surface and believed that the friction coefficient is similar to that between the two walls of a wing crack (Rawling et al. 2002; Dixon et al. 2007; Zhang 2013). However, the presence of water reduces the friction coefficient of this microstructure, explaining why water has a significant degradation effect on foliated rocks. For example, completely dry and water-free montmorillonite has a friction coefficient that can reach approximately 0.8, while the friction

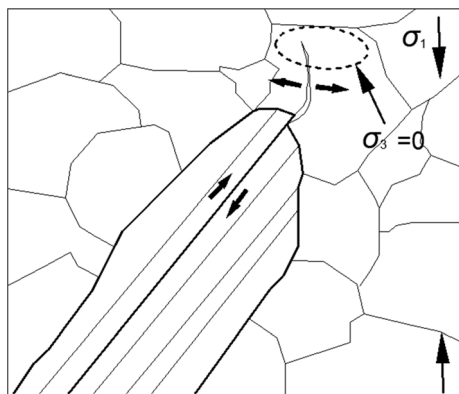


Fig. 5 Dislocation slip of flaky minerals

coefficient of saturated montmorillonite is only 0.18 under the same conditions (Dixon et al. 2007).

Given the weak plane angle at $\alpha = 45^\circ$, the shear stress of the dislocation slip on the cleavage plane reaches its maximum value (Kronenberg et al. 1990). A low friction coefficient will cause dislocation slip to occur under low shear stress, resulting in microscopic expansion (Rawling et al. 2002). This provides a reasonable explanation for the earliest volume expansion of the specimen at a medium foliation angle ($\alpha = 30^\circ\text{--}45^\circ$). In the linear elastic deformation stage, scholars found that the mica tip region and the tip of the wing crack have similar stress fields (Gottschalk et al. 1990).

After the compressive stress of the specimen reaches σ_{ci} , the dislocation slip initiation mode produces two types of cracks, namely shear cracks along the mica cleavage plane and tensile cracks near the plate-granular minerals. At the end of the mica tip, $\sigma_3 = 0$ is the critical condition for the extension of these tensile cracks (Diederichs et al. 2004). Therefore, the confining pressure will inhibit the extension of such cracks and improve the compressive strength of the specimen.

Furthermore, as the density of dislocations increases, a significant number of cracks obliquely crossing the cleavage plane at a low angle will form (Hallbauer et al. 1973). Then, the continued accumulation of these cracks will gradually form dislocation walls (Shea et al. 1993). The boundary of the plastic kink zone is the product of the further evolution of the dislocation wall, and the mechanism of this process remains unclear. However, scholars generally consider that plastic kinks are based on the secondary deformation of high-density dislocations in flaky minerals (Gay et al. 1974; Christoffersen et al. 1993; Mares et al. 1993).

2.1.2 Plastic Kink

According to the direction of the plastic kink, the kink belt is divided into left and right kinks (Hörz 1970; Dunham et al. 2011). This paper utilizes the right kink of mica, which causes crack germination, as an example to summarize and analyze its significance. There are two modes of initiation of the plastic kink, namely Type I initiation in the mica and Type II initiation near plate-granular minerals. The kink zone boundary (KBB) in the plastic kink Type I initiation

mode (Fig. 6a) is the dislocation wall formed by high-density dislocation slip. Generally, the width of the kink belt (w) is 0.1–10 μm (Mares et al. 1993; Shea et al. 1993), and both sides of the mica cleavage surface inside the kink belt tend to slide relatively.

Near the boundary of the kink zone, the mica will undergo crystal plastic deformation along the kink direction. In addition, the mica located outside the KBB will deflect at a small angle, which is generally less than 5° . When this plastic deformation becomes excessively large, it will cause cracks between the mica crystals (Bell et al. 1986), resulting in the formation of intergranular tension cracks (cr). It is worth noting that the boundary of the kink band may have a curve with a certain curvature rather than a consistently straight line (Bell et al. 1986; Yin et al. 2016). In other words, the β value of KBB on the same side may vary within a certain range. With the development of the Type I initiation mode into the later stage, a local stress concentration appears in the horizontal axis of the mica, causing cracks in the grain boundaries of plate-granular minerals or the initiation of adjacent plate-granular minerals (Type II). To date, the mechanical micromechanism of this type of crack initiation is still unclear. Nevertheless, several scholars (Olsson et al. 1976; Rawling et al. 2002) stated that cracks caused by a kink in the microscopic image have a shape that is similar to that of the sliding wing crack. Hence, crack initiation is speculated to be a form of tensile mechanism (Fig. 6b).

In the severely damaged area of the compression specimen, the stress state of mica is more complex, and complicated kink shapes may be generated, such

as the conjugate kink (Kronenberg et al. 1990) and hexagonal kink (Silk et al. 1961). Additionally, the weak surface angle α will affect the kink shape and the proportion of flaky minerals with kink deformation. Gay et al. (1974) found that when $\alpha = 5^\circ$, two pairs of conjugates usually experience kink deformation, in which the left or right kink appears when $\alpha = 5^\circ$ – 15° . When $\alpha > 15^\circ$, dislocation slip is more common than plastic kinks. Rawling et al. (2002) observed that the kink deformation near the failure surface of the specimen with (a) $\alpha = 0^\circ$ accounted for more than 90%, (b) $\alpha = 45^\circ$ had no kink near the failure surface, and (c) $\alpha = 90^\circ$ accounted for less than 1%. As the stress increases and when the stress generated by the plastic kink exceeds the strength of the mica, both transverse fracture and failure of the mica will be observed.

2.1.3 Fracture Failure

According to previous studies on the fracture behavior of mica, the new defects caused by fracture failure are divided into pores formed by mica cleavage fractures (v), intergranular tension cracks (cr), and splits near plate-granular minerals (Kronenberg et al. 1990; Shea et al. 1993; Rawling et al. 2002) (Fig. 7). Among these, the width of mica in the short axis direction of v and cr can reach the micron level (Shea et al. 1993). As the stress increases, the mica in specimens with $\alpha = 90^\circ$ usually undergoes widespread fracture.

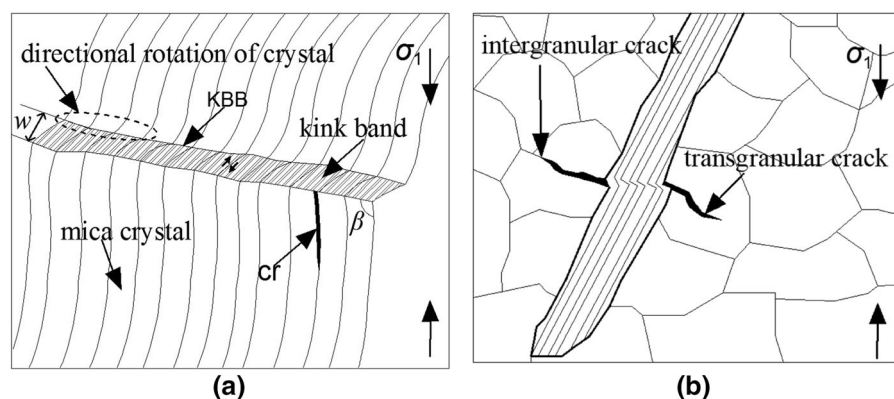


Fig. 6 Plastic kink of flaky minerals (KBB—the kink zone boundary, w —the width of the kink belt, cr—intergranular tension cracks, β —the angle between the kink zone boundary and the cleavage plane of the flaky mineral), **a** Type I; **b** Type II

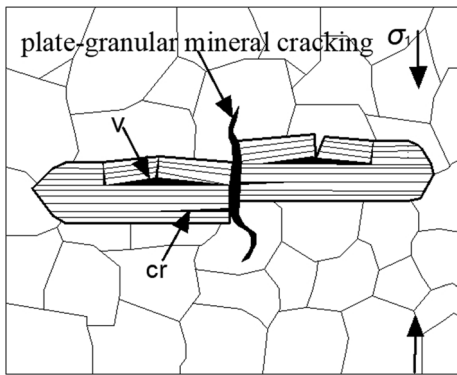


Fig. 7 Fracture failure of flaky minerals (v—mica cleavage fractures, cr—intergranular tension cracks)

2.2 Control of Directional Microcracks

In addition to the crack germination caused by the three deformation mechanisms of mica, new cracks may also be generated at the tips of the original defects, such as flaky mineral intergranular cracks, intragranular cracks of plate-granular minerals, and boundary cracks of plate-granular minerals. According to the sliding wing crack and Griffith theory, the original defect will produce tensile cracking behavior during the compression process of the specimen.

Based on the length of the defect, the radius of curvature at the end, and whether there is a slip mechanism, tensile cracks caused by original defects are divided into T-1 and T-2 (Fig. 8a-b) (Olsson et al. 1976; Rawling et al. 2002; Diederichs et al. 2004). To a certain extent, these two kinds of tension cracks alleviate the stress concentration at the end of the defect. The local critical condition for the expansion of tensile cracks is $\sigma_3 = 0$. Generally, these tensile cracks have the characteristics of simple shapes, long extensions and smooth crack surfaces. Among these two

types, the T-1 type, commonly found in brittle rocks under compressive stress, is recognized as a classic sliding initiation mechanism. The wing crack is deflected in the direction of maximum principal stress. The T-1 type usually occurs when the defect has perceptible long and short axes, sharp ends, and relative slippage on the upper and lower walls, such as directional microcracks. Approximately spherical defects, typically intragranular original defects of plate-granular minerals, tend to produce T-2 cracking, characterized by the absence of slip of the original defects.

With increasing stress, the limit length of the sliding crack extension that typically starts is 1–1.5 times the major axis size of the original defect. When the extension of the wing crack reaches its limit, the end of the initial defect will form another concentration of shear stress. Then, quasi-coplanar secondary cracks (S-1) or oblique secondary cracks (S-2) are generated (Sagong et al. 2002), which can be summarized as the shear initiation mode (Fig. 8c). Compared with the cracks initiated by tension, such shear-induced cracks normally extend a shorter distance and have more complex shapes (Yin et al. 2016). Most of the directional microcracks are distributed along the edge of the mica, and the direction of the other cracks is irregular.

Directional microcracks greatly contribute to the anisotropy of rock due to their nonuniform distribution and directional arrangement. It is worth noting that in the compression process of foliated rocks, the effect of directional microcracks on crack initiation depends on the loading direction. When the principal compressive stress is perpendicular to the microcrack surfaces, tensile cracks are unlikely to arise at the ends of the microcracks due to the lack of shear stress on the microcrack surfaces. In this case, the microcracks lose

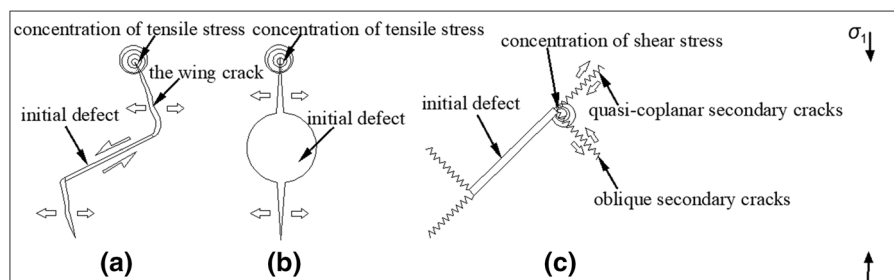


Fig. 8 Crack initiation at the tips of original defects (Sagong et al. 2002; Diederichs et al. 2004). **a** T-1 type; **b** T-2 type; **c** S-1 type and S-2 type

their leading role in the damage of the foliated rock. When the principal compressive stress obliquely intersects with the microcrack surfaces, new cracks are prone to appear following the T-1 initiation mechanism, especially at $\alpha = 30^\circ$ and the stress threshold for the initiation of new cracks is lower. Therefore, when $\alpha = 30^\circ$, foliated rocks tend to have lower crack initiation stress (Zhang et al. 2011).

Yin et al. (2020) analyzed the theory of fracture mechanics and the theory of maximum circumferential stress. They demonstrated that when the maximum principal stress and the macro weak plane are obliquely close to 30° , the directional microcracks control the initiation of the schist. Likewise, Rawling et al. (2002) pointed out that directional microcracks significantly impact the anisotropy and compressive strength of foliated rocks and have a significant “guide effect” on damage accumulation. In the compression process of the specimen, some adopted CT scanning technology to confirm that cracks are easier to generate, expand, and aggregate on the weak surface and eventually evolve into a macrofracture surface (Ma et al. 2020).

2.3 Influence of Water and Confining Pressure

Under the influence of water and confining pressure, the T-1 initiation of the original defect will change to a great extent. Under water lubrication, the friction coefficient between the two wall surfaces of the sliding crack is significantly reduced, making the relative slip more likely to occur under lower stress. As a result, it leads to an earlier stress concentration at the tip. Moreover, the increase in pore water pressure makes the tensile stress concentration at the front edge of the fracture more evident (Yang et al. 2018). Saturated specimens of foliated rock begin to initiate cracks earlier than those of dry specimens; that is, the physical and mechanical action of water under a specific microstructure reduces the σ_{ci} of foliated rocks, making the rock material more dangerous.

In contrast, since the critical condition of tensile wing crack extension is difficult to achieve, the initiation of tensile cracks is suppressed under the influence of a high confining pressure. During this time, a higher number of new cracks are generated in the end shear stress concentration area through the shear initiation mode. High confining pressure inhibits the initiation of wing cracks in the microstructure.

Restricted initiation of tensile cracks caused by high confining pressure leads to an increase in σ_{ci} of the foliated rock, which enhances the safety margin of the rock material. When water and confining pressure factors are coupled, their joint effect significantly reduces the deflection angle of wing cracks and suppresses the development of wing cracks. Furthermore, the expansion rate of the crack tip tends to be balanced, and the three-dimensional fracture propagation mode and the macroscopic fracture shape of the rock are changed (Yang et al. 2018).

3 Crack Propagation Mode

When the stress exceeds σ_{ci} , the specimen enters the crack propagation stage characterized by the initiation of grain boundary cracks and dominant intragranular cracks. Connecting two adjacent cracks or mica requires plate-granular minerals to penetrate the nearby plates, and these areas are often called rock bridges. Once cracks start at the flake minerals or at the end of the defect, the cracks will continue to propagate mainly in the rock bridge area (Fig. 9). It is worth noting that the crack propagation direction is approximately parallel to the direction of the maximum principal stress (Zhang et al. 2011). The intragranular cracks halt when they reach the plate-granular mineral boundary and are generally shorter in length. The grain boundary cracks can extend a longer distance; however, they halt or go around when encountering large plate-granular minerals. The intragranular cracks and grain boundary cracks tend to evolve into

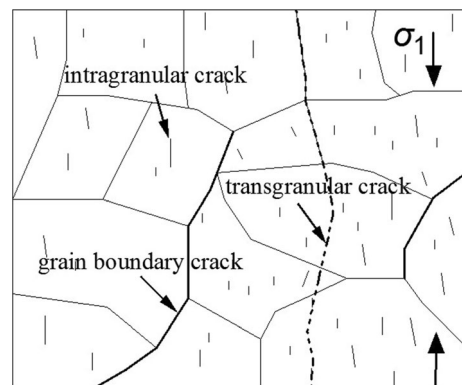


Fig. 9 Cracks in the rock bridges area

transgranular cracks, which will form in the crack aggregation stage.

There is extensive literature on the propagation mode of cracks through rock bridges. Sagong et al. (2002) summarized nine modes of crack propagation based on various experimental observations. Their study analyzed the factors affecting the different propagation modes, which included the angle between the maximum principal stress and the defect, the distance between the defects, the coplanarity of defects, and the continuity of defects.

According to the shape of the crack and the range of the fracture zone, the propagation mode can be divided into Types I, II, and III. In Type I propagation, elongated grain boundary tensile cracks usually penetrate the rock bridge (Fig. 10a). Occasionally, Z-shaped grain boundary cracks whose extending direction is approximately parallel to the direction of the maximum principal stress can be observed (Fonseka et al. 1985). This situation generally corresponds to a specimen with a small angle, wherein α is often 0° – 15° .

In the rock bridge area of Type II propagation, many grain boundary cracks and intragranular cracks are present (Fig. 10b). Subsequently, a microfracture zone in the rock bridge area (Rawling et al. 2002) develops along the mica cleavage plane. At this time, the crack becomes a fast path for crack propagation (Gottschalk et al. 1990), and this mode is commonly found in specimens with a medium angle (α often in the range 15° – 75°). In Type III propagation, large numbers of grain boundary cracks and intragranular cracks in the rock bridge region develop extensively, and wider fracture zones appear (Fig. 10c). Meanwhile, mica or microdefects whose long axis direction is approximately horizontal hinder crack propagation

(Shea et al. 1993; Rawling et al. 2002), and the above propagation mechanism generally occurs at large angles (α often in the range 75° – 90°) in specimens.

Comparing the three propagation modes, the plate-granular minerals in the vertical propagation mode will produce the most extensive grain boundary cracks and intragranular cracks (Rawling et al. 2002), followed by the oblique propagation mode. This phenomenon is consistent with the research findings that the fracture surface of the specimen with a large angle between the weak surface and the maximum principal stress has the largest fractal dimension. The fractal dimension of the small-angle specimen is the smallest, and the medium angle is centered (Carrillo et al. 2015; Xu et al. 2020).

4 Crack Aggregation Mode

When the stress reaches σ_{cd} , the unstable cracks begin to expand; that is, the cracks of the specimen enter the aggregation stage. In this period, the grain boundary cracks and intragranular cracks continue to expand and cross the mineral boundary (Zhang et al. 2011). The formation of transgranular cracks, following high-density intragranular cracks, requires a high energy provided by external work. Therefore, transgranular cracks hardly appear in plate-granular minerals unless under high stress level conditions and mainly occur in the crack aggregation stage (Diederichs et al. 2004).

The aggregation mode of cracks is closely related to the density of cracks near the fracture surface (Hallbauer et al. 1973). According to the width and density of the cracks of the specimen failure zone, it is divided into Types I, II, and III crack aggregation modes. In the Type I aggregation mode, the specimen produces

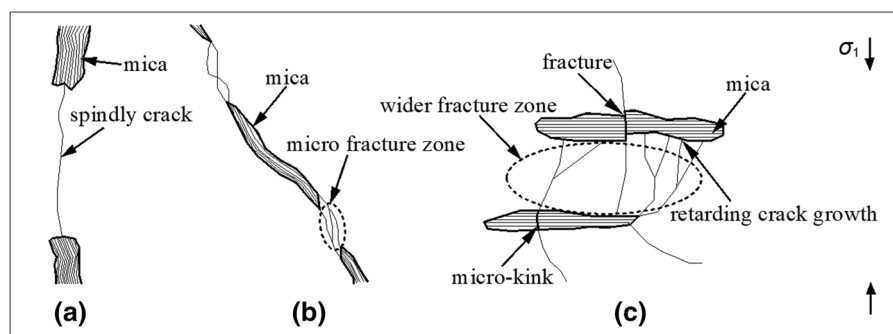


Fig. 10 Propagation mode of cracks. **a** Type I; **b** Type II; **c** Type III

the fewest cracks, the failure zone has the smallest limit width (Shea et al. 1993), and tensile failure usually occurs. Generally, the Type I aggregation mode is found in specimens with a small angle (Fig. 11a). A type II aggregation mode is generated in medium-angle specimens, accompanied by more cracks and rougher fracture surfaces (Fig. 11b). A type III aggregation mode is generated in large-angle specimens, such as for $\alpha = 90^\circ$ (Fig. 11c). Compared with the other aggregation types of specimens, the specimen sample corresponding to the Type III aggregation mode usually has the largest width of the failure zone and the greatest density of cracks.

The aggregation mode of cracks has a good correlation with the toughness and brittleness of the specimen. More specifically, Types I, II, and III aggregation modes correspond to the brittleness, transition, and toughness of the curves observed in the stress–strain curve (Mares et al. 1993; Shea et al. 1993). Additionally, the continuity of mica has a strong relationship with the toughness and brittleness of the specimen. Shea et al. (1993) defined linear mica continuity (*LMC*) and found that along the increase in *LMC* of the specimen of $\alpha = 45^\circ$, higher *LMC* will cause a trend in which strength decreases and ductility increases. In their study, all samples with $LMC_{\max} < 35\%$ in $\alpha = 45^\circ$ specimens incurred brittle fractures, and those with $LMC_{\max} > 60\%$ suffered ductile failures.

Different opinions exist on the microscopic factors that control the accumulation of cracks before the macroscopic fracture of foliated rocks. Studies have found that mica controls crack aggregation and the development of macroscopic fractures (Wong et al.

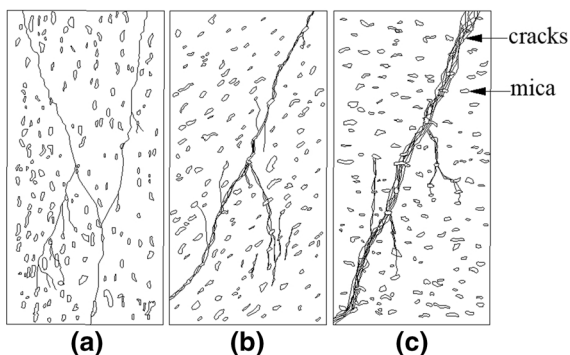


Fig. 11 Schematic diagram of the aggregation mode of cracks. **a** Type I; **b** Type II; **c** Type III

1985; Gottschalk et al. 1990; Rawling et al. 2002). In contrast, Shea et al. (1993) underlined that primary cracks primarily affect the crack aggregation mode and macrofractures. Analyzing these differences may shed light on their link to the density of mica. For example, Diederichs et al. (2004) showed that a small amount of mica reduces the strength of the specimen, but high-density mica can inhibit unstable crack growth and increase the in situ strength ratio.

5 Conclusion and Prospects

5.1 Conclusion

By comparing and analyzing the research of domestic and foreign scholars on the microscopic characteristics of foliated rocks, five conclusions are obtained through summary and induction.

1. After the compressive stress of the specimen reaches σ_{ci} , the deformation behavior of flaky minerals includes dislocation slip, plastic kinking, and fracture failure, which cause progressively brittle failure in the vicinity of flaky minerals. The initiation of directional microcracks plays a vital role in increasing the accumulation of damage in a specific direction.
2. During the stable crack propagation stage, the characteristics are defined by the initiation of grain boundary cracks and the dominant intragranular cracks. Additionally, the development direction of cracks is approximately parallel to the maximum principal stress. Meanwhile, mica or microdefects with long axis directions that are approximately horizontal hinder crack propagation.
3. During the unstable crack aggregation stage, crack aggregation mainly occurs. Based on the crack density and limit width on the failure surface of the specimen, there are three types of aggregation modes, specifically the brittleness, transition, and toughness curve shapes monitored in the stress–strain curve.
4. Distinct microscopic characteristics lead to differences in the initiation, propagation, and aggregation modes of cracks, which are the different mechanisms of microscopic failure that affect the roughness of the corresponding failure surface of the specimen. Finally, these modes cause the

fractal dimension of the specimen with various weak surface angles to be slightly different.

5. The weak surfaces composed of flake minerals and directional microcracks have a significant “guide effect” on the initiation, propagation, and aggregation of cracks. Eventually, this effect will cause the compressed foliated rocks to appear with a more significant anisotropy.

5.2 Prospects

First, the microscopic test is typically destructive. It is challenging to observe the continuous deformation and the progressive development of cracks for the same microstructure. Artificial damage to the sample is inevitable during the preparation process of the microscopic specimen. Second, the initial damage randomly distributed inside the rock specimen has a more considerable impact on the development of cracks. Finally, under the influence of external factors such as water and confining pressure, the anisotropic behaviors of crack development change significantly. However, the depth of the existing studies remains insufficient. Therefore, the following points must be further studied and researched in the future:

- (1) High-precision nondestructive detection technologies, such as CT scanning, acoustic emission, and 3D-DIC systems, can be used to continuously observe the anisotropic characteristics of cracks in microstructures.
- (2) Establishing a refined numerical model of foliated rock that better reflects the characteristics of the actual microstructure involving the flaky mineral morphology, the spatial distribution of flaky minerals and directional microcracks, could more accurately describe the law of the anisotropic development of cracks.
- (3) Considering the influence of water and confining pressure on the numerical model, the appropriate contact models and mesomechanical parameters should be selected, and the mechanism of the external factors on the progressively brittle failure of the compressed foliated rocks should be studied.

Acknowledgements This research is financially supported by the Nanhu Scholars Program of Xinyang Normal University and the Natural Science Foundation of China (Grant No. 41807240).

The author gratefully acknowledges the financial support provided by them.

Author contributions XY wrote original draft preparation and finished all drawing; AZ helped polish the manuscript; XZ changed the format of the manuscript. All authors have read and agreed to the published version of the manuscript.

Funding The Natural Science Foundation of China (Grant No. 41807240).

Declarations

Conflict of interest We declare that we have no conflict of interest.

References

- Bell I, Wilson C, McLaren A et al (1986) Kinks in mica: role of dislocations and (001) cleavage. *Tectonophysics* 127(1):49–65
- Carrillo LMG, Sulem J, Seyedi D et al (2015) Analysis of long-term anisotropic convergence in drifts excavated in callovo-oxfordian claystone. *Rock Mech Rock Eng* 49(1):97–114
- Christoffersen R, Kronenberg AK (1993) Dislocation interactions in experimentally deformed biotite. *J Struct Geol* 15(9):1077–1095
- Diederichs M, Kaiser P, Eberhardt E (2004) Damage initiation and propagation in hard rock during tunneling and influence of near-face stress rotation. *Int J Rock Mech Min Sci* 41(5):785–812
- Dixon TH, Moore JC (2007) *The seismogenic zone of subduction thrust faults*. Columbia University Press, New York
- Dunham R, Crider J, Burmester R et al (2011) Geometry, microstructures, and magnetic fabrics of kink bands in the darrington phyllite, northwestern Washington, USA: processes within fixed-hinge kinking. *J Struct Geol* 33(11):1627–1638
- Fisher G (1970) The application of ionic equilibria to metamorphic differentiation: an example. *Contrib Miner Petrol* 29(2):91–103
- Fonseka G, Murrell S, Barnes P (1985) Scanning electron microscope and acoustic emission studies of crack development in rocks. *Int J Rock Mech Min Sci Geomech Abstr* 22(5):273–289
- Gay N, Weiss L (1974) The relationship between principal stress directions and the geometry of kinks in foliated rocks. *Tectonophysics* 21(3):287–300
- Gottschalk R, Kronenberg A, Russell J et al (1990) Mechanical anisotropy of gneiss: failure criterion and textural sources of directional behavior. *J Geophys Res* 95(B13):21613–21634
- Hallbauer D, Wagner H, Cook N (1973) Some observations concerning the microscopic and mechanical behaviour of quartzite specimens in stiff, triaxial compression tests. *International Journal of Rock Mechanics and Mining Sciences & Geomechanics Abstracts* 10(6):713–726

- Hörz F (1970) Static and dynamic origin of kink bands in micas. *J Geophys Res* 75(5):965–977
- Kanaori Y, Kawakami S, Yairi K (1991) Microstructure of deformed biotite defining foliation in cataclasite zones in granite, central japan. *J Struct Geol* 13(7):777–785
- Kronenberg A, Kirby S, Pinkston J (1990) Basal slip and mechanical anisotropy of biotite. *J Geophys Res* 95(B12):19257–19278
- Ma J, Niu X, Xiong C et al (2020) Experimental investigation of the physical properties and microstructure of slate under wetting and drying cycles using micro-CT and ultrasonic wave velocity tests. *Sensors* 20(17):4853
- Mares V, Kronenberg A (1993) Experimental deformation of muscovite. *J Struct Geol* 15(9):1061–1075
- Olsson WA, Peng SS (1976) Microcrack nucleation in marble. *Int J Rock Mech Min Sci Geomech Abstr* 13(2):53–59
- Passchier CW, Trouw RAJ (2005) *Microtectonics*. Springer, New York
- Powell D (1977) Crystalline plasticity and solid state flow in metamorphic rocks. *Mineral Mag* 41(319):422–422
- Rawling G, Baud P, Wong T (2002) Dilatancy, brittle strength, and anisotropy of foliated rocks: experimental deformation and micromechanical modeling. *J Geophys Res*, 107(B10), ETG-8
- Sagong M, Bobet A (2002) Coalescence of multiple flaws in a rock-model material in uniaxial compression. *Int J Rock Mech Min Sci* 39(2):229–241
- Shea WT, Kronenberg AK (1993) Strength and anisotropy of foliated rocks with varied mica contents. *J Struct Geol* 15(9):1097–1121
- Silk E, Barnes R (1961) The observation of dislocations in mica. *Acta Metall* 9(6):558–562
- Wang JX (2014) Research for the anisotropy of quartz mica schist and its effect on the stability of the surrounding rock. Chengdu University of Technology, Chengdu
- Wang ZQ, Yan EC (2015) Influence of material composition and structural characteristics of rock on free-thaw damage and deterioration of schist. *Chin J Geotechn Eng* 37(S2):86–90 (in Chinese)
- Wong TF, Biegel R (1985) Effects of pressure on the micromechanics of faulting in san marcos gabbro. *J Struct Geol* 7(6):737–749
- Xu G, He C, Chen Z et al (2020) Transversely isotropic creep behavior of phyllite and its influence on the long-term safety of the secondary lining of tunnels. *Eng Geol* 278:105834
- Yang L, Mei J, Li SC et al (2018) Research on the initiation and propagation modes of 3-D crack under hydro-mechanical coupling. *Adv Eng Sci* 50(6):174–183 ((in Chinese))
- Yin S, Ding WL, Sun YX et al (2016) Shale uniaxial compressive failure property and the affecting factors of UCS. *Earth Sci Front* 23(2):75–95 ((in Chinese))
- Yin XM, Yan EC, Wang LN et al (2020) Anisotropy of quartz mica schist based on quantitative extraction of fabric information. *Bull Eng Geol Env* 79(5):2439–2456
- Yu QF (2016) Research on deformation features and support technology of surrounding rock in pinal schist tunnel during construction. China University of Geosciences, Wuhan
- Zhang L (2013) An experimental study on frictional sliding of fault rocks from longmenshan fault zone under hydrothermal conditions. Institute of Geology, China Earthquake Administration, Beijing
- Zhang XP, Wong LNY, Wang SJ et al (2011) Engineering properties of quartz mica schist. *Eng Geol* 121(3):135–149

Publisher's Note Springer Nature remains neutral with regard to jurisdictional claims in published maps and institutional affiliations.